Applied Physics Letters

Impurity band assisted carrier relaxation in Cr doped topological insulator Bi$_2$Se$_3$ ⊘

Jian Tu; Yafei Zhao ✉ ⓘ ; Xiaoqian Zhang; Zhonghui Nie; Yao Li; Yilin Zhang; Ion Cristian Edmond Turcu; Luca Poletto; Fabio Frassetto ⓘ ; Xuezhong Ruan; Wenbin Zhong; Xuefeng Wang ⓘ ; Wenqing Liu; Yu Zhang; Rong Zhang; Yongbing Xu ✉ ; Liang He ✉ ⓘ

Check for updates

View Online Export Citation

24 June 2024 09:10:45

AIP Publishing

Impurity band assisted carrier relaxation in Cr doped topological insulator Bi_2Se_3

Jian Tu,[1] Yafei Zhao,[1,a)] Xiaoqian Zhang,[1] Zhonghui Nie,[2] Yao Li,[1] Yilin Zhang,[1] Ion Cristian Edmond Turcu,[1] Luca Poletto,[3] Fabio Frassetto,[3] Xuezhong Ruan,[1] Wenbin Zhong,[1] Xuefeng Wang,[1] Wenqing Liu,[1,4] Yu Zhang,[5] Rong Zhang,[1] Yongbing Xu,[1,6,a)] and Liang He[1,a)]

AFFILIATIONS

[1] Jiangsu Provincial Key Laboratory of Advanced Photonic and Electronic Materials, School of Electronic Science and Engineering and Collaborative Innovation Center of Advanced Microstructures, Nanjing University, Nanjing 210093, China

[2] MIIT Key Laboratory of Advanced Display Materials and Devices, Institute of Optoelectronics and Nanomaterials, College of Materials Science and Engineering, Nanjing University of Science and Technology, Nanjing 210094, China

[3] National Research Council Institute of Photonics and Nanotechnologies, Padova 35131, Italy

[4] Department of Electronic Engineering, Royal Holloway University of London, Egham TW20 0EX, United Kingdom

[5] Central Laser Facility, STFC Rutherford Appleton Laboratory, Didcot OX11 0QX, United Kingdom

[6] York-Nanjing Joint Center in Spintronics, Department of Electronic Engineering, The University of York, York YO10 5DD, United Kingdom

[a)] Authors to whom correspondence should be addressed: heliang@nju.edu.cn; njnjzhao@nju.edu.cn; and ybxu@nju.edu.cn

ABSTRACT

Topological insulators (TIs) with unique band structures have wide application prospects in the fields of ultrafast optical and spintronic devices. The dynamics of hot carriers plays a key role in these TI-based devices. In this work, using the time- and angle-resolved photoemission spectroscopy technique, the relaxation process of the hot carriers in Cr-doped Bi_2Se_3 has been systematically studied since the ferromagnetic TI is one of the key building blocks for next-generation spintronics. It is found that electronic temperature (T_e) and chemical potential (μ) decrease faster with the increase in the Cr doping concentration. Similarly, the lifetime (τ) of the excited electrons also decreases with more Cr doped into Bi_2Se_3. The results suggest a mechanism of impurity band-assisted carrier relaxation, where the impurity band within the bulk bandgap introduced by Cr doping provides significant recombination channels for the excited electrons. This work directly illustrates the dynamic process of the photon-generated carriers in Cr-doped Bi_2Se_3, which is expected to promote the applications of $(Bi_{1-x}Cr_x)_2Se_3$ in photoelectric devices.

Published under license by AIP Publishing. https://doi.org/10.1063/5.0039440

TIs are a class of quantum materials featuring a bandgap in their bulk and unique Dirac-like metallic states on the surface, which have a broad application prospects in the fields of ultrafast optical and spintronic devices.[1–3] The performance of these devices depends on the dynamics of the hot carriers in TIs, which can be observed directly by TR-ARPES.[4–6] So far, a number of works have been carried on illustrating the recovery process of the excited electrons in TIs due to various mechanisms such as phonons assisted,[7,8] surface states assisted,[9] and electron–electron scattering assisted.[10,11]

Recently, numerous works have reported that doping with transition metals can introduce novel physical phenomena into TIs, such as the quantum anomalous Hall effect (QAHE),[12] giant magneto-optical Kerr effect,[13] and chiral Majorana fermions.[14] In addition, doping

with transition metals changes the band structure of TIs by weakening the surface states, increasing the bulk bandgap, and introducing impurity bands, which may also affect the carrier relaxation. However, this effect has not been systematically studied experimentally although it is crucial for the application of TIs in photoelectric devices.

In this work, a series of $(Bi_{1-x}Cr_x)_2Se_3$ ($x = 0 \sim 0.074$) samples were grown by molecular beam epitaxy (MBE). Then, the dynamic processes of the excited electrons in $(Bi_{1-x}Cr_x)_2Se_3$ are directly studied by TR-ARPES. It is found that as the Cr doping concentration increases, the relaxation rate of T_e and μ increases and τ of the excited electrons decreases. This has been attributed to the mechanism of impurity band-assisted carrier relaxation. The impurity band within the bulk bandgap introduced by Cr provides additional recombination

channels for the excited electrons. This work provides direct insight into the relaxation mechanisms of the Cr-doped TIs and, therefore, has profound implications for future works exploring the potential of these materials for photoelectric devices.

Bi_2Se_3 and $(Bi_{1-x}Cr_x)_2Se_3$ ultrathin films were grown on fluorophlogopite $[KMg_3(AlSi_3O_{10})F_3]$ substrates by MBE. Compared with conventional epitaxy, van der Waals epitaxy (VDW) growth significantly relaxes the stringent conditions of lattice match between the substrate and the epitaxial layer.[15–17] Moreover, atomically flat fluorophlogopite with a pseudohexagonal layered structure is suitable for VDW epitaxy growth of layered material due to no dangling bonds associated with the surface.[18,19] The Cr dopants were evaporated simultaneously with Bi and Se atoms and deposited on fluorophlogopite at 200 °C. The growth was carried out in an Se-rich environment with a nominal Se to Bi ratio of 20:1, which is beneficial for reducing the Se vacancy defects.[20] The Cr doping concentration ($x = 0.013–0.074$) is determined by Cr deposition flux and x-ray photoelectron spectroscopy (XPS). Samples were transferred into the ARPES chamber through a high vacuum tube ($<3.0 \times 10^{-9}$ mbar) to ensure clean surfaces. The band structure of the $(Bi_{1-x}Cr_x)_2Se_3$ films measured by static ARPES (He-I, 21.2 eV) at room temperature is shown in Fig. 1. It is found that the bulk valence band (BVB), topological surface state (TSS), and bulk conduction band (BCB) can be clearly distinguished in undoped Bi_2Se_3. However, the TSS weakens and the bulk bandgap increases with the increase in the Cr doping concentration. When the Cr doping concentration is increased to $x = 0.074$, the surface states cannot be observed at all in the band structure. This is consistent with previous results.[21,22]

TR-ARPES measurements were performed using a pump-probe scheme. The laser pulse with a wavelength of 800 nm (~1.55 eV) and a repetition rate of 1 kHz is split into two beams. One beam is used as the pump light to stimulate the sample, and the other is used for high harmonic generation (HHG).[23–26] The 13th harmonic extreme ultraviolet (EUV) at ~20.15 eV has been chosen as the probe light.[27] A detailed description of the HHG system can be found in our previous work.[28] The overall energy resolution is 190 meV, and the time resolution is 60 fs. Pump light was s polarized, which was maintained at 0.21 mJ/cm² during the measurements. Saturation effects could be excluded with this pump influence (supplementary material S1). Probe light was p polarized, and the flux of the probe pulse was chosen to minimize the space charge effect. All the experiments were carried out at room temperature.
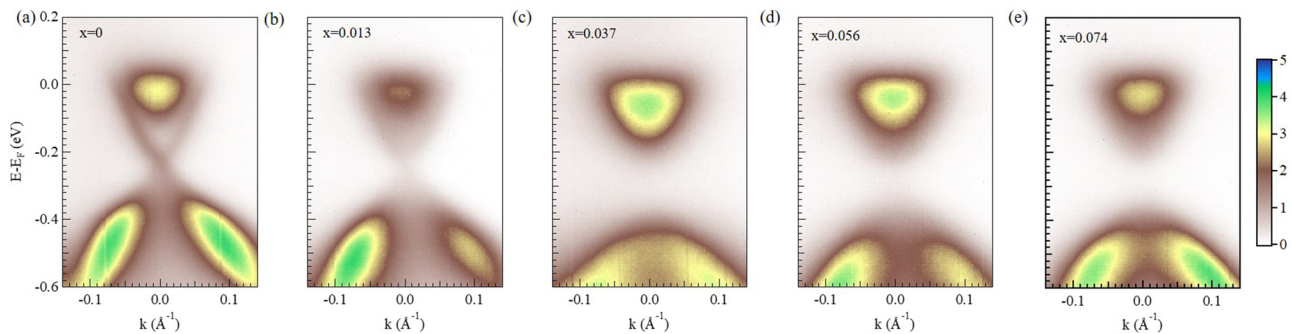
Figures 2(a)–2(c) demonstrate the differential band structures (obtained by subtracting the band structure at −0.2 ps) of $(Bi_{1-x}Cr_x)_2Se_3$ ($x = 0.013$) obtained by EUV after pumping. Red and blue represent the increased and decreased electrons at different E-k positions, respectively. It is found that the intensity above the Fermi level is strongest at 0.7 ps because of the increase in T_e and the relaxation of electrons at a higher energy level.[29] Then, it reduces at 1.5 ps due to the relaxation of excited electrons assisted by phonons. It should be noted that the influence of transport can be neglected in our case since the thicknesses (~13 nm) of samples are smaller than the penetration depth of pump light (50 nm) and the diameter of the pump spot (1 mm) is larger than that of the probe spot (0.5 mm).[9] The band structure almost recovers to the un-excited state at 10 ps, as shown in Fig. 2(c). Figures 2(e)–2(g) and 2(i)–2(k) show the differential band structures of higher doped samples with $x = 0.056$ and 0.074, respectively. A similar dynamic process of excited electrons could be seen in these three samples. Namely, after the pump light, electrons are excited above the Fermi level, then quickly fall back around the Fermi level, and finally return to its original state.[8]

The dynamic process of the hot electrons around the Fermi level after pumping can be quantified by the Fermi–Dirac (FD) distribution convoluted with a Gauss distribution,

$$I(E,t) = A(t) \int_{-\infty}^{\infty} \left[F(\varepsilon, T_e(t), \mu(t))D(\varepsilon) \right] G(E - \varepsilon, \sigma)]d\varepsilon. \quad (1)$$

Here, I represents the energy dispersion curve (EDC) as a function of delay time, F is the FD distribution, and T_e and μ denote the electron temperature and chemical potential, respectively. G is the Gauss distribution to take the overall energy resolution of the system (mainly depends on EUV) into consideration through σ. A and D are the scale factor[30] and the product of the photoemission matrix element and the density of states, respectively.[31] Due to the complexity to determine D,[32] in the fitting process, a narrow range around the Γ point (± 0.01 Å^{-1} around the center) has been integrated to extract the leading edge of the EDCs [as shown in Figs. 2(d), 2(h), and 2(l)]. In this way, D can be treated as a constant for every single sample[33] (supplementary material S2). Although this simple treatment neglects the fine structure in D, it is helpful to compare the dynamic processes of different samples quantitatively.

Figure 2(d) demonstrates EDCs of $x = 0.013$ at different delay times. It is found that the EDC at 0.7 ps (black line) shifts to higher

FIG. 1. The band structures of a series of $(Bi_{1-x}Cr_x)_2Se_3$ with $x = 0$ (a), 0.013 (b), 0.037 (c), 0.056 (d), and 0.074 (e). The color bar represents the density of electrons at the energy level.
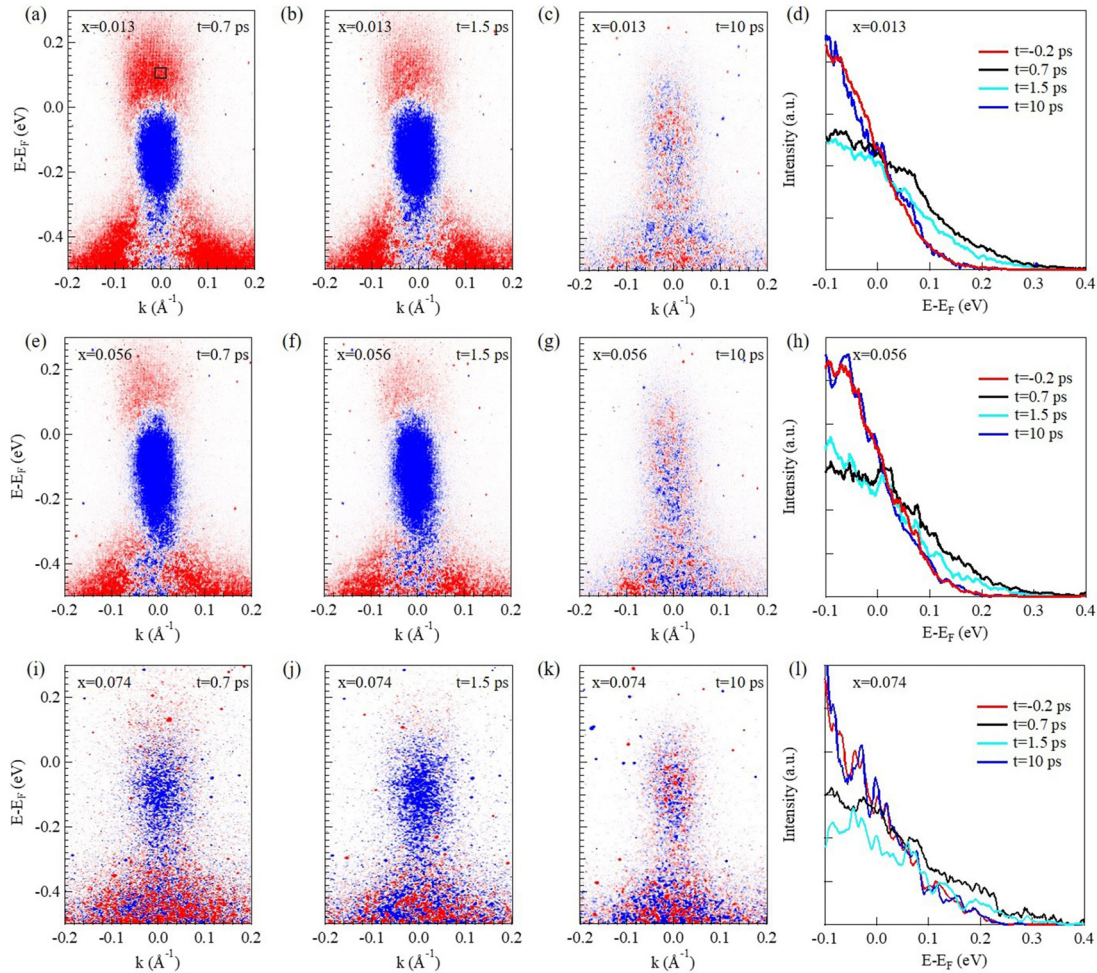
FIG. 2. (a)–(c) Differential band structures of $(Bi_{1-x}Cr_x)_2Se_3$ (x = 0.013) around the Γ point at t = 0.7 ps, 1.5 ps, and 10 ps, respectively, acquired by subtracting the band structure of t = −0.2 ps. (e)–(g) and (i)–(k) show the differential band structures of $(Bi_{1-x}Crx)_2Se_3$ with x = 0.056 and 0.074, respectively. (d), (h), and (l) show the EDCs integrated between ± 0.01 Å⁻¹ around the Γ point at different delay times with x = 0.013, 0.056, and 0.074, respectively. Using Fermi–Dirac distribution convoluted with a Gaussian function, T_e and $\Delta\mu$ can be extracted.

energy compared to −0.2 ps (red line), which means that T_e and μ of the former are higher, due to the thermalization of electrons in the CB after absorbing the energy from pump photons. The EDC at 1.5 ps shows intermediate features compared with the EDCs at 0.7 ps and −0.2 ps since the energy exchange between electrons and phonons assists the relaxation of excited electrons. At 10 ps after the arrival of pump photons, the excited electrons almost recombine with the holes and the sample recovers to the state before excited. EDCs at the same delay time of x = 0.056 [Fig. 2(h)] and 0.074 [Fig. 2(l)] demonstrate a similar recovery process.

Moreover, T_e and μ as a function of delay time with different x values are extracted using Eq. (1) to fit the EDCs, as shown in Figs. 3(a) and 3(b). The T_e value of x = 0 reveals a quick relaxation from the peak value to around 500–590 K and maintains around that temperature within the detection window [Fig. 3(a)]. The reason is the weak coupling of phonons and surface electrons.[33] $\Delta\mu$ quickly decreases after pumping due to the excitation of electrons around the Fermi level

to the higher energy level and then increases as for the relaxation of electrons at a higher energy level and the increase in T_e.[7] At the final stage, $\Delta\mu$ recovers to zero by electron-phonon interaction. It should be noted that $\Delta\mu$ vs delay time at the final stage does not satisfy the exponential decay function at a low Cr doping concentration, suggesting that the activity of phonons at the surface of low doping Bi_2Se_3 is weak.[33] Interestingly, with the increase in x (x = 0.013–0.074), T_e and $\Delta\mu$ recover more quickly, which also demonstrates the ability of Cr doping to assist the relaxation of excited electrons.

In order to reveal τ of the excited carriers, a black box was fixed at 0.1 eV above the Fermi level [as shown in Fig. 2(a)] to indicate the integral domain. The integral intensities as a function of delay time for various $(Bi_{1-x}Cr_x)_2Se_3$ films are shown in Fig. 3(c). After pumping light, electrons are immediately excited above the Fermi level and then quickly fall back around the Fermi level.[34] After that, electrons relax to its original state through the electron-phonon coupling process.[8] Meanwhile, the electron relaxation rate of undoped Bi_2Se_3 is slower
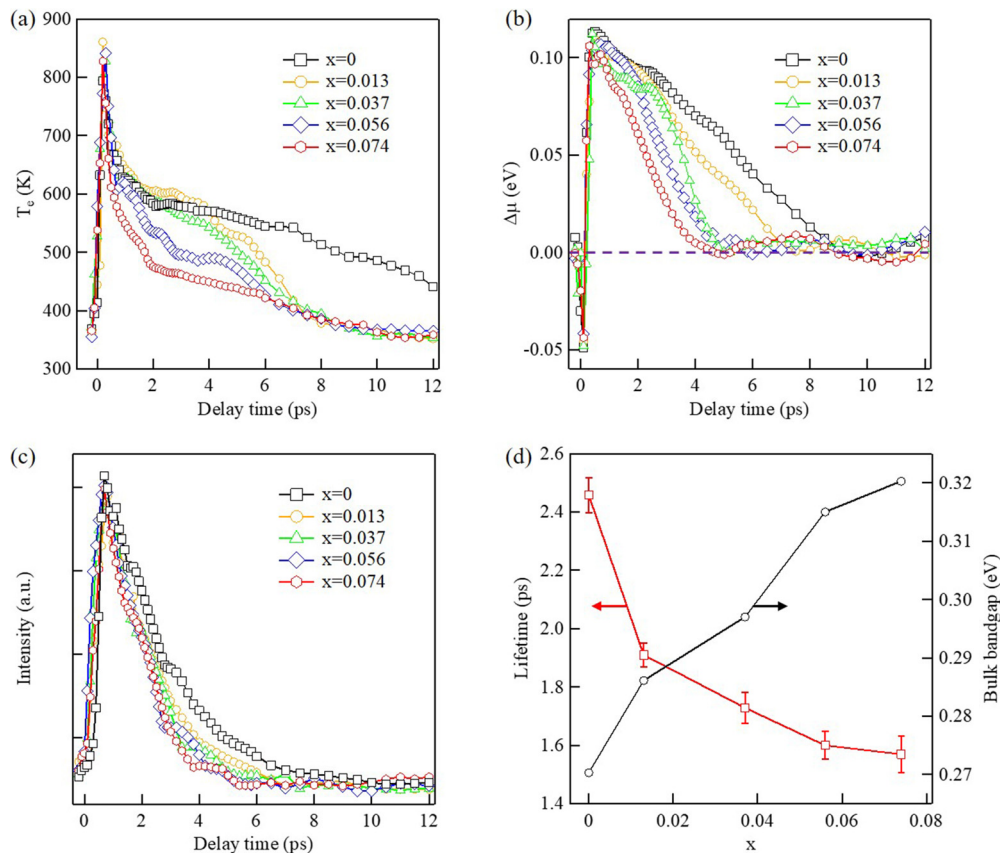
FIG. 3. (a) T_e and (b) $\Delta\mu$ as a function of the delay time with different x values. T_e and $\Delta\mu$ recover more quickly with the increase in the Cr doping concentration. (c) Normalized integral intensities within the black boxes in Fig. 2(a), as a function of the delay time for different samples. (d) The lifetime (τ) of the excited electrons and bulk bandgap as the function of Cr doped concentration (x).

than that of Cr doped Bi_2Se_3. Namely, Cr doping reduces the τ of excited electrons. With the use of single exponential decay function to fit the curves in Fig. 3(c), τ of excited electrons can be extracted as a function of x, as shown in Fig. 3(d). It is found that τ decreases monotonically with the increase in doping concentration x.

Two factors have been reported to influence τ of the excited electrons in TIs.[4,7] First, the presence of surface states provides additional paths (2 and 3) for the relaxation of electrons through the coupling of the TSS and BCB [Fig. 4(a)].[4] Thus, higher Cr-doped samples should have longer τ, because of the disappearance of the TSS.[35] Second, doping Cr enlarges the bulk bandgap (the method to extract the bulk bandgap is described in the supplementary material, S3) as shown in Fig. 3(d). This is consistent with our calculated band structure using VASP package (supplementary material S4). However, the reports demonstrate that the enlarged bulk bandgap can only increase τ of the excited carriers,[22] which again contradicts this work.

To explain our results, we propose here another mechanism to assist carrier relaxation through the impurity band. The band structures of $(Bi_{1-x}Cr_x)_2Se_3$ are shown in Fig. S4. It is found that the impurity band (mainly composed of Cr-d states) appears at the bottom of the BCB and the top of the BVB after doping Cr, as shown by the red dashed curves in Figs. 4(b) and S4. Moreover, as more Cr atoms are

doped into the lattice, the density of states of the impurity band increases. Due to the existence of the impurity band, the excited electrons can move to the impurity band at the bottom of the BCB directly. Then, they can jump down to the impurity band above the top of the BVB (path 3) or the BVB (path 4), as shown in Fig. 4(b). Thus, the impurity band provides additional recombination channels, which assists the relaxation of the exited carriers.[36,37] It should be noted that the impurity band can hardly be detected by EUV-based ARPES,[36,37] but can be observed by STS and resonant ARPES.[38]

According to Shockley-Read-Hall recombination theory, considering n-type conduction and low optical injection situation in this work, the recombination rate (R_I) of excess carriers passing through path 2, path 3, and path 4 can be written as $R_I = (C_2 N_I + C_3 N_I + C_4 N_I)\delta_p$, quantitatively. C_2, C_3, and C_4 are constants representing the hole capture cross section of the impurity band. N_I is the number of trap centers, which can be estimated by the integral of the density of states of the impurity band. δ_p is the number of excess holes, which is relevant to the absorption coefficient[39] and the pump fluence. In this work, pump fluence is constant, and the influence of Cr doping on the absorption coefficient can be neglected since the bandgap change is within 60 meV. Thus, δ_p can be treated as a constant. Meanwhile, the recombination rate of the bulk (path 1) (R_B) can be written as $R_B = C_1 N_B \delta_p$. C_1 is a constant

24 June 2024 09:10:45
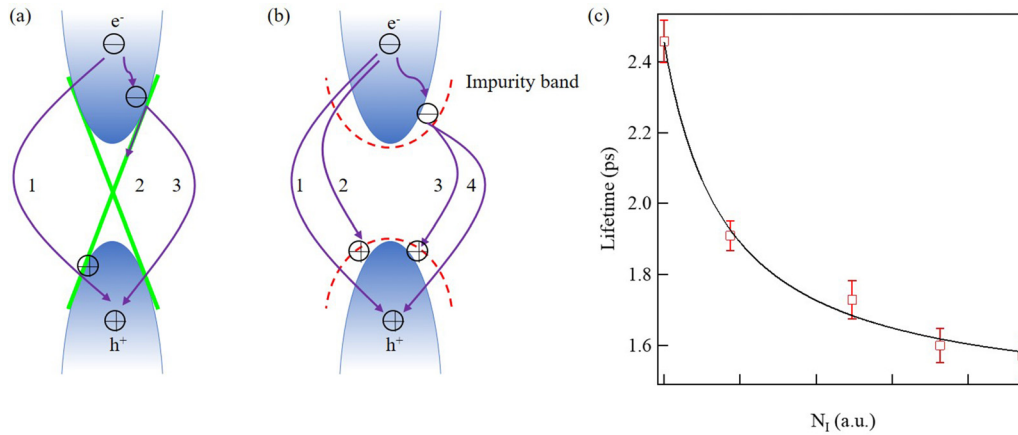
FIG. 4. Mechanism diagram of the non-equilibrium carrier recombination processes of (a) undoped and (b) Cr-doped Bi_2Se_3. The results show that the impurity band can provide additional carrier recombination channels. Green lines represent the surface states. (c) The carrier lifetime (τ) as a function of the density of states of the impurity band. The results show that τ of hot carriers reduces with the increase in the density of states of the impurity band.

representing the hole capture cross section of the bulk band. N_B is the density of states around the Fermi level.

Here, τ of the excited carriers is proportional to $1/R$, so it can be written as

$$\tau = \frac{1}{R_I + R_B} = \frac{1}{(C_2 + C_3 + C_4)N_I + C_1 N_B}. \quad (2)$$

Furthermore, τ can be simplified as $\tau = \frac{1}{C_2' N_I + C_1'}$ because C_1, C_2, C_3, and C_4 are constants and N_B is approximately linear in N_I (supplementary material S5). Here, a constant τ_0 has been added as $\tau = \tau_0 + \frac{1}{C_2' N_I + C_1'}$, and the fitting results of τ vs impurity band density are shown in Fig. 4(c). The results suggest that τ shortens with the increase in the density of states of the impurity band. We have also performed the integration within a larger region, and the results demonstrate similar tendency of lifetime vs Cr doping concentration (supplementary material S6). Thus, the impurity band induced by the Cr doping provides additional recombination paths, overcoming the previous two factors (the vanishing of the surface state and the increase in the bulk bandgap), and effectively reducing τ of the hot electrons.

In summary, we have systematically studied the dynamic process of photoexcited carriers in high-quality $(Bi_{1-x}Cr_x)_2Se_3$ with different Cr doping concentrations by TR-ARPES. It is found that as the Cr doping concentration increases, T_e and μ decrease faster. Second, τ of the excited electrons decreases with the increase in the Cr doping concentration. This has been attributed to the relaxation mechanism through the impurity band induced by Cr doping, which provides additional recombination paths. This work has found an effective method to regulate the carrier lifetime in TIs through doping, which may promote their applications in photoelectric devices.

See the supplementary material for the exclusion of the saturation effect in the experiments, the simplification of Eq. (1), the method to extract the bandgap, the theoretical band structure of Cr-doped Bi_2Se_3, the derivation process of Eq. (2), and the intensity within a larger region vs delay time.

AUTHORS' CONTRIBUTIONS

J.T. and Y.F.Z. contributed equally to this work.

DATA AVAILABILITY

The data that support the findings of this study are available from the corresponding author upon reasonable request.

REFERENCES

[1]H. Steinberg, D. R. Gardner, Y. S. Lee, and P. Jarillo-Herrero, "Surface state transport and ambipolar electric field effect in Bi_2Se_3 nanodevices," Nano Lett. **10**, 5032 (2010).
[2]J. G. Checkelsky, Y. S. Hor, R. J. Cava, and N. P. Ong, "Bulk band gap and surface state conduction observed in voltage-tuned crystals of the topological insulator Bi_2Se_3," Phys. Rev. Lett. **106**, 196801 (2011).
[3]J. W. McIver, D. Hsieh, H. Steinberg, P. Jarillo-Herrero, and N. Gedik, "Control over topological insulator photocurrents with light polarization," Nat. Nano **7**, 96 (2012).
[4]J. A. Sobota, S. Yang, J. G. Analytis, Y. L. Chen, I. R. Fisher, P. S. Kirchmann, and Z. X. Shen, "Ultrafast optical excitation of a persistent surface-state population in the topological insulator Bi_2Se_3," Phys. Rev. Lett. **108**, 117403 (2012).
[5]J. A. Sobota, S. L. Yang, A. F. Kemper, J. J. Lee, F. T. Schmitt, W. Li, R. G. Moore, J. G. Analytis, I. R. Fisher, P. S. Kirchmann, T. P. Devereaux, and Z. X. Shen, "Direct optical coupling to an unoccupied Dirac surface state in the topological insulator Bi_2Se_3," Phys. Rev. Lett. **111**, 136802 (2013).
[6]M. Neupane, S. Y. Xu, Y. Ishida, S. Jia, B. M. Fregoso, C. Liu, I. Belopolski, G. Bian, N. Alidoust, T. Durakiewicz, V. Galitski, S. Shin, R. J. Cava, and M. Z. Hasan, "Gigantic surface lifetime of an intrinsic topological insulator," Phys. Rev. Lett. **115**, 116801 (2015).
[7]Y. H. Wang, D. Hsieh, E. J. Sie, H. Steinberg, D. R. Gardner, Y. S. Lee, P. Jarillo-Herrero, and N. Gedik, "Measurement of intrinsic Dirac fermion cooling on the surface of the topological insulator Bi_2Se_3 using time-resolved and angle-resolved photoemission spectroscopy," Phys. Rev. Lett. **109**(12), 127401 (2012).

[8] J. A. Sobota, S. L. Yang, D. Leuenberger, A. F. Kemper, J. G. Analytis, I. R. Fisher, P. S. Kirchmann, T. P. Devereaux, and Z. X. Shen, "Distinguishing bulk and surface electron-phonon coupling in the topological insulator Bi_2Se_3 using time-resolved photoemission spectroscopy," Phys. Rev. Lett. **113**, 157401 (2014).

[9] F. Freyse, M. Battiato, L. V. Yashina, and J. Sánchez-Barriga, "Impact of ultrafast transport on the high-energy states of a photoexcited topological insulator," Phys. Rev. B **98**(11), 115132 (2018).

[10] C. Jozwiak, J. A. Sobota, K. Gotlieb, A. F. Kemper, C. R. Rotundu, R. J. Birgeneau, Z. Hussain, D. H. Lee, Z. X. Shen, and A. Lanzara, "Spin-polarized surface resonances accompanying topological surface state formation," Nat. Commun. **7**, 13143 (2016).

[11] C. Cacho, A. Crepaldi, M. Battiato, J. Braun, F. Cilento, M. Zacchigna, M. C. Richter, O. Heckmann, E. Springate, Y. Liu, S. S. Dhesi, H. Berger, P. Bugnon, K. Held, M. Grioni, H. Ebert, K. Hricovini, J. Minar, and F. Parmigiani, "Momentum-resolved spin dynamics of bulk and surface excited states in the topological insulator Bi_2Se_3," Phys. Rev. Lett. **114**(9), 097401 (2015).

[12] C.-Z. Chang, J. S. Zhang, X. Feng, J. Shen, Z. C. Zhang, M. H. Guo, K. Li, Y. B. Ou, P. Wei, L.-L. Wang, Z.-Q. Ji, Y. Feng, S. H. Ji, X. Chen, J. F. Jia, X. Dai, Z. Fang, S.-C. Zhang, K. He, Y. Y. Wang, L. Lu, X.-C. Ma, and Q.-K. Xue, "Experimental observation of the quantum anomalous hall effect in a magnetic topological insulator," Science **340**(6129), 167 (2013).

[13] W. K. Tse and A. H. MacDonald, "Giant magneto-optical Kerr effect and universal Faraday effect in thin-film topological insulators," Phys. Rev. Lett. **105**(5), 057401 (2010).

[14] X.-L. Qi, T. L. Hughes, and S.-C. Zhang, "Chiral topological superconductor from the quantum Hall state," Phys. Rev. B **82**(18), 184516 (2010).

[15] H. Li, J. Cao, W. Zheng, Y. Chen, D. Wu, W. Dang, K. Wang, H. Peng, and Z. Liu, "Controlled synthesis of topological insulator nanoplate arrays on mica," J. Am. Chem. Soc. **134**, 6132 (2012).

[16] K. H. M. Chen, H. Y. Lin, S. R. Yang, C. K. Cheng, X. Q. Zhang, C. M. Cheng, S. F. Lee, C. H. Hsu, Y. H. Lee, M. Hong, and J. Kwo, "Van der Waals epitaxy of topological insulator Bi_2Se_3 on single layer transition metal dichalcogenide MoS_2," Appl. Phys. Lett. **111**, 083106 (2017).

[17] X. F. Kou, L. He, F. X. Xiu, M. R. Lang, Z. M. Liao, Y. Wang, A. V. Fedorov, X. X. Yu, J. S. Tang, G. Huang, X. W. Jiang, J. F. Zhu, J. Zou, and K. L. Wang, "Epitaxial growth of high mobility Bi_2Se_3 thin films on CdS," Appl. Phys. Lett. **98**, 242102 (2011).

[18] Y. J. Liu, M. Tang, M. M. Meng, M. Z. Wang, J. X. Wu, J. B. Yin, Y. B. Zhou, Y. F. Guo, C. W. Tan, W. H. Dang, S. Y. Huang, H. Q. Xu, Y. Wang, and H. L. Peng, "Epitaxial growth of ternary topological insulator Bi_2Te_2Se 2D crystals on mica," Small **13**, 1603572 (2017).

[19] W. Zheng, T. Xie, Y. Zhou, Y. Chen, W. Jiang, S. Zhao, J. Wu, Y. Jing, Y. Wu, G. Chen, Y. Guo, J. Yin, S. Huang, H. Q. Xu, Z. Liu, and H. Peng, "Patterning two-dimensional chalcogenide crystals of Bi_2Se_3 and In_2Se_3 and efficient photodetectors," Nat. Commun. **6**, 6972 (2015).

[20] L. He, X. F. Kou, and K. L. Wang, "Review of 3D topological insulator thin-film growth by molecular beam epitaxy and potential applications," Phys. Status Solidi RRL **7**, 50 (2013).

[21] M. Liu, J. Zhang, C. Z. Chang, Z. Zhang, X. Feng, K. Li, K. He, L. L. Wang, X. Chen, X. Dai, Z. Fang, Q. K. Xue, X. Ma, and Y. Wang, "Crossover between weak antilocalization and weak localization in a magnetically doped topological Insulator," Phys. Rev. Lett. **108**(3), 036805 (2012).

[22] M. Brahlek, N. Bansal, N. Koirala, S. Y. Xu, M. Neupane, C. Liu, M. Z. Hasan, and S. Oh, "Topological-metal to band-insulator transition in $(Bi_{1-x}In_x)_2Se_3$ thin films," Phys. Rev. Lett. **109**(18), 186403 (2012).

[23] C. Grazioli, C. Callegari, A. Ciavardini, M. Coreno, F. Frassetto, D. Gauthier, D. Golob, R. Ivanov, A. Kivimäki, B. Mahieu, B. Bučar, M. Merhar, P. Miotti, L. Poletto, E. Polo, B. Ressel, C. Spezzani, and G. De Ninno, "CITIUS: An infrared-extreme ultraviolet light source for fundamental and applied ultrafast science," Rev. Sci. Instrum. **85**, 023104 (2014).

[24] R. Cucini, T. Pincelli, G. Panaccione, D. Kopic, F. Frassetto, P. Miotti, G. M. Pierantozzi, S. Peli, A. Fondacaro, A. De Luisa, A. De Vita, P. Carrara, D. Krizmancic, D. T. Payne, F. Salvador, A. Sterzi, L. Poletto, F. Parmigiani, G. Rossi, and F. Cilento, "Coherent narrowband light source for ultrafast photoelectron spectroscopy in the 17–31 eV photon energy range," Struct. Dyn. **7**(1), 014303 (2020).

[25] M. Ferray, A. L'Huillier, X. F. Li, L. A. Lomprk, G. Mainfray, and C. Manus, "Multiple-harmonic conversion of 1064 nm radiation in rare gases," J. Phys. B: At. Mol. Opt. Phys. **21**, L31–L35 (1988).

[26] R. Haight, J. A. Silberman, and M. I. Ulie, "Novel system for picosecond photoemission spectroscopy," Rev. Sci. Instrum. **59**, 1941 (1988).

[27] M. P. Seah and W. A. Dench, "Quantitative electron spectroscopy of surfaces: A standard data base for electron inelastic mean free paths in solids," Surf. Interf. Anal. **1**(1), 2 (1979).

[28] Z. Nie, I. C. E. Turcu, Y. Li, X. Q. Zhang, L. He, J. Tu, Z. Q. Ni, H. F. Xu, Y. Q. Chen, X. Q. Ruan, F. Frassetto, P. Miotti, N. Fabris, L. Poletto, J. Wu, Q. S. Lu, C. Liu, T. Kampen, Y. Zhai, W. Q. Liu, C. Cacho, X. F. Wang, F. Q. Wang, Y. Shi, R. Zhang, and Y. B. Xu, "Spin-ARPES EUV beamline for ultrafast materials research and development," Appl. Sci. **9**, 370 (2019).

[29] I. Gierz, F. Calegari, S. Aeschlimann, M. Chavez Cervantes, C. Cacho, R. T. Chapman, E. Springate, S. Link, U. Starke, C. R. Ast, and A. Cavalleri, "Tracking primary thermalization events in graphene with photoemission at extreme time scales," Phys. Rev. Lett. **115**(8), 086803 (2015).

[30] W. S. Fann, R. Storz, H. W. K. Tom, and J. Bokor, "Direct measurement of nonequilibrium electron-energy distributions in subpicosecond laser-heated gold films," Phys. Rev. Lett. **68**(18), 2834 (1992).

[31] S. Hüfner, *Photoelectron Spectroscopy: Principles and Applications* (Springer Science & Business Media, Germany, 2013).

[32] Y. Ishida, T. Togashi, K. Yamamoto, M. Tanaka, T. Taniuchi, T. Kiss, M. Nakajima, T. Suemoto, and S. Shin, "Non-thermal hot electrons ultrafastly generating hot optical phonons in graphite," Sci. Rep. **1**, 64 (2011).

[33] A. Crepaldi, F. Cilento, B. Ressel, C. Cacho, J. C. Johannsen, M. Zacchigna, H. Berger, P. Bugnon, C. Grazioli, I. C. E. Turcu, E. Springate, K. Kern, M. Grioni, and F. Parmigiani, "Evidence of reduced surface electron-phonon scattering in the conduction band of Bi_2Se_3 by nonequilibrium ARPES," Phys. Rev. B **88**(12), 121404(R) (2013).

[34] H. Soifer, A. Gauthier, A. F. Kemper, C. R. Rotundu, S. L. Yang, H. Xiong, D. Lu, M. Hashimoto, P. S. Kirchmann, J. A. Sobota, and Z. X. Shen, "Band-resolved imaging of photocurrent in a topological insulator," Phys. Rev. Lett. **122**(16), 167401 (2019).

[35] Z. Y. Wang, T. Zhou, T. Jiang, H. Y. Sun, Y. Y. Zang, Y. Gong, J. H. Zhang, M. Y. Tong, X. N. Xie, Q. H. Liu, C. Y. Chen, K. He, and Q. K. Xue, "Dimensional crossover and topological nature of the thin films of a three-dimensional topological insulator by band gap engineering," Nano Lett. **19**(7), 4627 (2019).

[36] K. Sumida, M. Kakoki, J. Reimann, M. Nurmamat, S. Goto, Y. Takeda, Y. Saitoh, K. A. Kokh, O. E. Tereshchenko, J. Güdde, U. Höfer, and A. Kimura, "Magnetic-impurity-induced modifications to ultrafast carrier dynamics in the ferromagnetic topological insulators $Sb_{2x}V_xTe_3$," New J. Phys. **21**(9), 093006 (2019).

[37] E. Papalazarou, L. Khalil, M. Caputo, L. Perfetti, N. Nilforoushan, H. Deng, Z. Chen, S. Zhao, A. Taleb-Ibrahimi, M. Konczykowski, A. Hruban, A. Wołoś, A. Materna, L. Krusin-Elbaum, and M. Marsi, "Unraveling the Dirac fermion dynamics of the bulk-insulating topological system Bi_2Te_2Se," Phys. Rev. Mater. **2**(10), 104202 (2018).

[38] V. N. Strocov, T. Schmitt, U. Flechsig, T. Schmidt, A. Imhof, Q. Chen, J. Raabe, R. Betemps, D. Zimoch, J. Krempasky, X. Wang, M. Grioni, A. Piazzalunga, and L. Patthey, "High-resolution soft x-ray beamline ADRESS at the Swiss Light Source for resonant inelastic x-ray scattering and angle-resolved photoelectron spectroscopies," J Synchrotron Radiat. **17**(5), 631 (2010).

[39] Y. Wang and S. Law, "Optical properties of $(Bi_{1-x}In_x)_2Se_3$ thin films," Opt. Mater. Express **8**(9), 2570 (2018).

24 June 2024 09:10:45